REVIEW OF DIFFRACTION AT THE LHC*

Robert Ciesielski

The Rockefeller University
1230 York Avenue, New York, NY 10065, USA

(Received December 7, 2015)

We present the review of the recent results on diffraction from the LHC.

DOI:10.5506/APhysPolBSupp.8.769
PACS numbers: 12.38.Qk, 13.85.–t, 13.85.Dz, 13.85.Lg

1. Introduction

In hadron–hadron scattering, a substantial fraction of the total cross section can be attributed to diffractive interactions, characterized by the presence of at least one non-exponentially suppressed large rapidity gap (LRG), *i.e.* a region of pseudorapidity η devoid of particles. The LRG is associated with a color-singlet exchange carrying the vacuum quantum numbers, commonly referred to as *Pomeron* exchange. Diffractive processes are classified as soft or hard, depending on the presence of a hard scale in the interaction.

Soft diffractive cross sections cannot be calculated within perturbative Quantum Chromodynamics (pQCD), and are commonly described by phenomenological models. Predictions of these models generally differ when extrapolated from Tevatron center-of-mass energies to LHC. Therefore, measurements of diffractive cross sections at the LHC provide a valuable input for understanding diffraction and improving its theoretical description. Together with the total and elastic cross section results, they are crucial for the proper modeling of the full final state of hadronic interactions in event generators, and the simulation of hadronic showers in cosmic ray physics.

Hard diffraction events are especially interesting because they can be studied in terms of pQCD, thus providing an opportunity to investigate the nature of the *Pomeron* in terms of quarks and gluons, and to establish a link between soft and hard regimes. Exclusive production of simple identified final states reveals an interesting connection between diffraction and the physics of heavy-ion collisions through the concept of saturation in the

* Presented at EDS Blois 2015: The 16$^{\text{th}}$ Conference on Elastic and Diffractive Scattering, Borgo, Corsica, France, June 29–July 4, 2015.

regime of high parton densities; it also offers the possibility for searches for beyond-Standard-Model phenomena or exotic particles, such as glueballs.

2. Total and elastic cross sections

TOTEM measured the total $\sigma_{\rm tot}$, elastic $\sigma_{\rm el}$ and total inelastic, $\sigma_{\rm inel} = \sigma_{\rm tot} - \sigma_{\rm el}$, hadronic pp cross sections at $\sqrt{s} = 7$ and 8 TeV, using data from special runs with the $\beta^* = 90$ m beam optics [1–4]. Elastic cross sections were obtained from the integrated and extrapolated differential $d\sigma/d|t|$ cross section, where $|t|$ is the four-momentum transfer squared at the proton vertex, in the region of $0.005 < |t| < 2.5$ GeV^2, with protons tagged in the TOTEM Roman Pot detectors located at $z = \pm 220$ m downstream of the CMS detector. The total pp cross section was obtained from the elastic scattering using the optical theorem. At 7 TeV, $\sigma_{\rm el} = 25.4 \pm 1.1$ mb, $\sigma_{\rm tot} = 98.6 \pm 2.2$ mb and $\sigma_{\rm inel} = 73.2 \pm 1.6$ mb were measured by TOTEM (luminosity-dependent method [1]), in agreement with the results of a similar measurement by ATLAS [5], $\sigma_{\rm el} = 24.0 \pm 0.6$ mb, $\sigma_{\rm tot} = 95.4 \pm 1.3$ mb, and $\sigma_{\rm inel} = 71.3 \pm 0.9$ mb, based on data with protons tagged in the ALFA detectors ($z = \pm 240$). These results were found to have a big impact on the phenomenological model predictions. An interesting summary of the evaluation of the predictions before and after including the LHC data can be found in Ref. [6].

TOTEM also measured elastic scattering at $\sqrt{s} = 8$ TeV using a high-statistics data sample [7]. With an unprecedented precision below 1%, an evidence for a non-exponential differential cross section was observed, and a purely exponential dependence was excluded with a significance greater than 7 standard deviations. Two extended parameterizations, with quadratic and cubic polynomials in the exponent, were found to be well compatible with the data. Another study was based on the data taken with the $\beta^* = 1000$ m optics, which allowed to reach $|t|$ values as low as $|t| \simeq 6 \times 10^{-4}$ GeV^2, and to observe the effects of Coulomb-nuclear interference [8]. A study of the phase of the hadronic amplitude is ongoing.

3. Soft diffractive cross sections

ATLAS has measured [9] the inclusive cross section as a function of the forward pseudorapidity gap, $\Delta\eta^{\rm F}$, defined as the distance of the most-forward-detected particle to the edge of the central detector ($|\eta| = 4.9$). The differential $d\sigma/d\Delta\eta^{\rm F}$ cross section at $\sqrt{s} = 7$ TeV (Fig. 1, left) in the region $\Delta\eta^{\rm F} > 3$ is dominated by the diffractive events, with an approximately

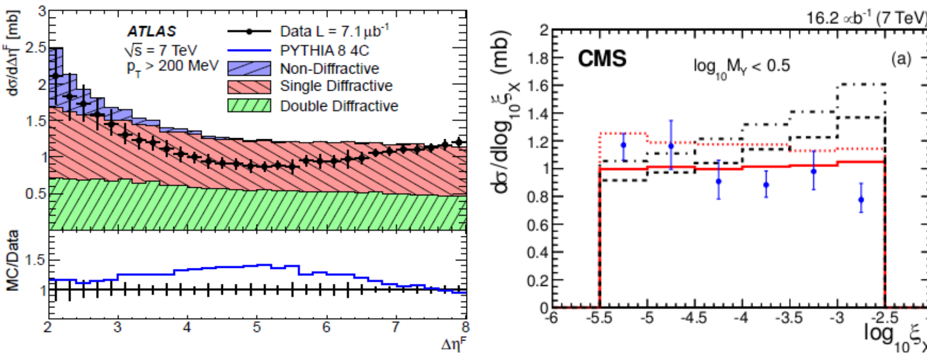

Fig. 1. Left: Differential cross section as a function of the forward rapidity gap, $\Delta\eta^{\mathrm{F}}$, measured by ATLAS, compared to the PYTHIA8 MC simulation. Right: Cross section $d\sigma/d\log_{10}\xi_X$ measured by CMS for $\log_{10} M_Y < 0.5$ (SD dominated), compared to PYTHIA8-4C, PYTHIA8-MBR, and PYTHIA6-Z2$*$ predictions.

equal contribution from the single-dissociation (SD, $pp \to Xp$ or $pp \to Yp$) and double-dissociation (DD, $pp \to XY$) diffraction processes, in which a low-mass dissociated system X or Y escapes undetected.

CMS has measured [10] the SD and DD cross sections at $\sqrt{s} = 7$ TeV, using the events with a forward or central pseudorapidity gap in the detector ($|\eta| < 4.7$). In the forward-gap sample ($\Delta\eta^{\mathrm{F}} > 3$), subsamples enhanced in SD and DD events were selected by requiring an absence or a presence of an energy deposit in the CASTOR calorimeter (located at $-6.6 < \eta < -5.2$, in the direction of the gap). This allowed to measure the differential cross sections as a function of $\xi_X = M_X^2/s$, in the range $-5.5 < \log_{10}\xi_X < -2.5$, for $\log_{10} M_Y < 0.5$ (dominated by SD), and $0.5 < \log_{10} M_Y < 1.1$ (dominated by DD), where M_X and M_Y correspond to diffractive masses (given in GeV). The cross sections were compared to MC predictions by PYTHIA8-4C, PYTHIA8-MBR and PYTHIA6-Z2$*$ (Fig. 1, right, for the SD-dominated sample), and PHOJET, QGSJET-II 03, QGSJET-II 04, EPOS (not shown). The data are able to distinguish between different diffractive models, favoring PYTHIA8-MBR [11] simulation. Similar conclusions may be drawn from the comparison to the differential cross section measured as a function of the width of the central pseudorapidity gap $\Delta\eta$ for $\Delta\eta > 3$, $\log_{10} M_X > 1.1$, and $\log_{10} M_Y > 1.1$ (DD dominated). The SD and DD cross sections integrated over the above three regions were used to extract the total SD and DD cross sections of $\sigma^{\mathrm{SD}} = 8.84 \pm 0.08(\mathrm{stat.})^{+1.49}_{-1.38}(\mathrm{syst.})^{+1.17}_{-0.37}(\mathrm{extrap.})$ mb and $\sigma^{\mathrm{DD}} = 5.17 \pm 0.08(\mathrm{stat.})^{+0.55}_{-0.57}(\mathrm{syst.})^{+1.62}_{-0.51}(\mathrm{extrap.})$ mb in the regions of $\xi < 0.05$ and $\Delta\eta > 3$, respectively (after an extrapolation by a factor of ~ 2 with PYTHIA8-MBR).

The SD cross section at $\sqrt{s} = 7$ TeV has been also measured by TOTEM [8], based on events with one proton in the Roman Pot detectors and the activity in the TOTEM T1 ($3.1 < |\eta| < 4.7$) or T2 ($5.3 < |\eta| < 6.5$) telescopes. The differential $d\sigma/d|t|$ cross section was measured in three ranges of diffractive masses, M_X, selected by different configurations of active T1 and T2 detectors. The cross section integrated over the entire accessible mass range, $3.4 < M_X < 1000$ GeV, was measured to be 6.5 ± 1.3 mb. TOTEM has also measured [12] the DD cross section of 120 ± 25 μb in the region of low diffractive masses $3.4 < M_X < 8$ GeV and $3.4 < M_Y < 8$ GeV detected in the T2 telescopes (and empty T1 detectors).

4. Hard diffraction

A striking feature of hard diffractive cross sections in hadron–hadron collisions is the observation of the pQCD factorization breaking, manifesting as a suppresion of diffractive cross sections at the Tevatron, by an order of magnitude, relative to the predictions based on HERA diffractive PDFs, see *e.g.* [13]. This suppresion, quantified by the so-called *rapidity gap survival probability*, is understood as due to additional soft multiparton interactions.

Obtaining results on hard diffraction at higher energies at the LHC has been hampered by a limited detector coverage of available rapidity space, which leads to difficulties in reconstructing large rapidity gaps and separating hard diffractive events from non-diffractive. *E.g.*, in the CMS analysis of SD dijets at $\sqrt{s} = 7$ TeV with the central CMS detector [14], diffractive events were selected in a limited region of the diffractive variable ξ (fractional proton momentum loss), $0.0003 < \xi < 0.002$, and a rapidity gap survival probability of 0.12 ± 0.05 (LO) and 0.08 ± 0.04 (NLO) was extracted, sensitive to the contribution from non-diffractive and DD backgrounds. A similar ongoing analysis at $\sqrt{s} = 8$ TeV, using common 2012 CMS+TOTEM data and the additional requirement that the scattered proton be detected in the TOTEM Roman Pot, has demonstrated good control of the background [15], and aims at measuring the cross section as a function of $|t|$ and other diffractive variables.

CMS has performed a study of events with a large rapidity gap in the η region between two jets at $\sqrt{s} = 7$ TeV [16]. The jet–gap–jet events were first observed by the CDF [17] and D0 [18], and the topology has been suggested as being sensitive to effects of the BFKL dynamics [19]. The Tevatron data were successfully described by models based on the NLO BFKL evolution equations [20,21], convoluted with the contribution from rescattering processes. Figure 2, left, shows the color-singlet-exchange (CSE) fractions, defined as a ratio of jet–gap–jet events to all dijet events, measured by CMS as a function of the second-leading jet p_{T}, compared to the results

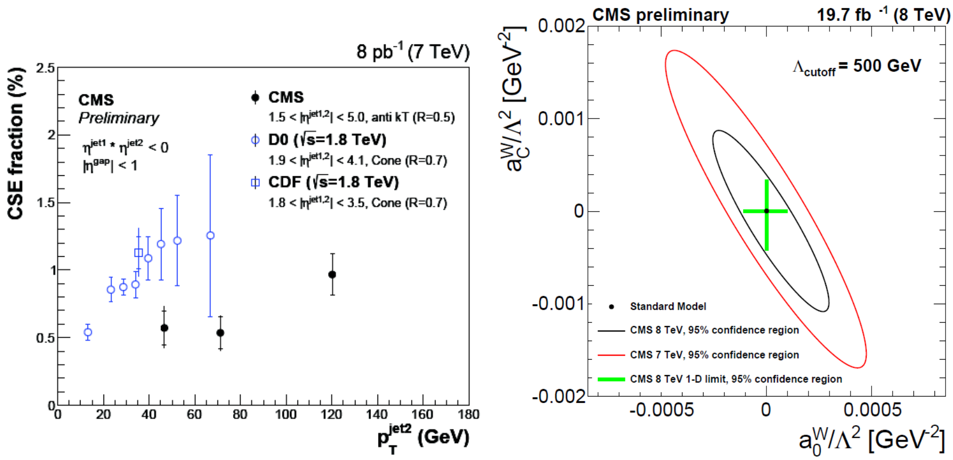

Fig. 2. Left: Color-singlet-exchange fractions measured by CMS at $\sqrt{s} = 7$ TeV as a function of the second leading jet p_T, compared to the Tevatron results. Right: CMS limits on anomalous quartic gauge couplings at $\sqrt{s} = 8$ TeV.

of CDF and D0. The data are a factor of two suppressed with respect to 1.8 TeV data, indicating stronger contribution from soft re-scattering processes at higher energy. A preliminary comparison to the predictions of Ref. [20] reveals that the modeling of re-scattering processes, which worked well at Tevatron energies, needs additional adjustments to describe the 7 TeV data.

The joined CMS and TOTEM runs at $\sqrt{s} = 13$ TeV in 2015, based on a larger data sample, will allow more hard diffraction measurements to be performed, to be further continued by the CT-PPS (collaboration between CMS and TOTEM on the Precision Proton Spectrometers) [22], and by the AFP (ATLAS Forward Physics) projects [23].

5. Exclusive processes

The central exclusive production in hadron–hadron collisions may proceed by photon–photon, Pomeron–Pomeron, or photon–Pomeron interactions. The photon–photon exchange allows to test QED predictions and search for beyond-Standard-Model physics. The $\mathbb{P}$–$\mathbb{P}$ exchange selects the $I^G(J^{PC}) = 0^+(\text{even})^{++}$ states and allows to study spectroscopy of isoscalar states (including glueballs). The γ–$\mathbb{P}$ exchange allows to study the $\gamma p \to Vp$ process (with $V = \rho, \phi, J/\psi, \Upsilon$), which exhibits a high sensitivity to the gluon distribution in the proton at very low Bjorken-x. At the LHC, it may be used to search for effects of gluon saturation.

ATLAS measured the cross section for the exclusive $\gamma\gamma \to l^+l^-$ production at $\sqrt{s} = 7$ TeV [24], for centrally produced high-p_{T} muons and electrons. The ratio of the cross sections, relative to the QED predictions, which have an uncertainty of about 2%, was measured to be about 80%, indicating a suppression due to soft re-scattering effects. CMS measured the cross section for the exclusive $\gamma\gamma \to W^+W^-$ production at $\sqrt{s} = 8$ TeV [25], and set the world-strongest limits on anomalous quartic gauge couplings (Fig. 2, right), which are a factor of 20 (100) better than the Tevatron (LEP) limits.

The first measurement of the $\mathbb{P}$–$\mathbb{P}$ induced production of $J/\psi + J/\psi$ and $J/\psi + \psi'$ pairs in pp collisions was performed by the LHCb [26], who found 57 $J/\psi + J/\psi$ and seven $J/\psi + \psi'$ candidates in events with four tracks and at least 3 muons. The cross section for the exclusive $J/\psi + J/\psi$ production was measured to be 24 ± 9 pb, in agreement with theoretical predictions.

LHCb also measured cross sections for the exclusive production of J/ψ and ψ' mesons at $\sqrt{s} = 7$ TeV [27], with dimuons at forward rapidities, $2 < y < 4.5$. The measured $d\sigma/dy$ cross sections favor NLO over LO QCD predictions, and agree with the models that include saturation effects. The J/ψ result was used to extract the cross section as a function of the photon–proton center-of-mass energy $W_{\gamma p}$. In the high-$W_{\gamma p}$ region ($400 < W_{\gamma p} < 1100$), the data are well described by the function W^{δ}, $\delta = 0.67$, extracted from the fit to the HERA data ($30 < W_{\gamma p} < 300$). ALICE measured the exclusive J/ψ production cross section in p–Pb collisions (with the lead-ion serving as the source of the photon), for the J/ψ in rapidity $2.5 < y < 4$ [28]. The cross section measured as a function of $W_{\gamma p}$ is compared to HERA results in Fig. 3, left. The parameters of the power-law fit to ALICE results are consistent with those of HERA, indicating no change in gluon behavior at the LHC energies compared to HERA. LHCb also measured the exclusive Υ production cross section at $\sqrt{s} = 7$ and 8 TeV [29], as a function of dimuon rapidity and $W_{\gamma p}$. In Fig. 3, right, the results are compared to the

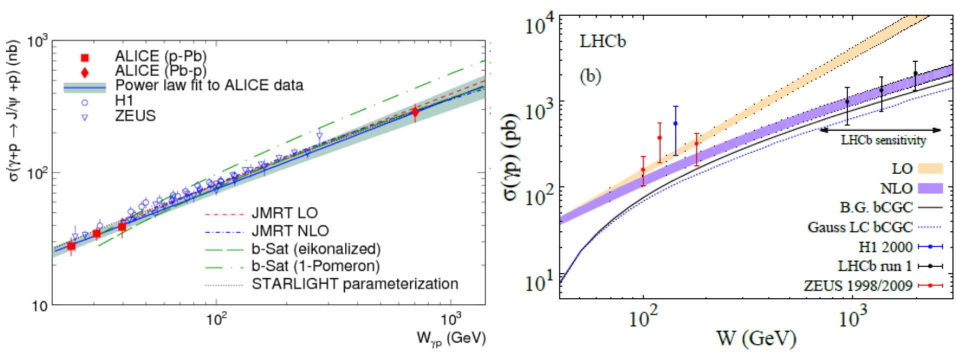

Fig. 3. Cross sections of exclusive vector-meson production measured as a function of $W_{\gamma p}$ for the (left) J/ψ meson by ALICE and (right) Υ meson by LHCb.

LO and NLO QCD predictions, favoring strongly the NLO calculations. For the future LHCb analyzes, the installation of HERSCHEL shower counters down to $\eta = \pm 9$ will greatly reduce the non-exclusive backgrounds.

The cross section of coherent J/ψ photoproduction was also measured in Pb–Pb collisions, in two rapidity intervals by ALICE [30, 31] and in one rapidity interval by CMS [32]. This process, with the lead-ion serving as both a source and a target, allows a study of nuclear gluon shadowing. The ALICE and CMS data agree with the models which include nuclear gluon shadowing employing the EPS09 parametrization. ALICE also measured photoproduction of ρ^0 in Pb–Pb collisions [33], which is well described by the STARLIGHT simulation using the Glauber model.

REFERENCES

[1] G. Antchev *et al.* [TOTEM Collaboration], *Eur. Phys. Lett.* **101**, 21002 (2013).

[2] G. Antchev *et al.* [TOTEM Collaboration], *Eur. Phys. Lett.* **101**, 21004 (2013).

[3] G. Antchev *et al.* [TOTEM Collaboration], *Eur. Phys. Lett.* **101**, 21003 (2013).

[4] G. Antchev *et al.* [TOTEM Collaboration], *Phys. Rev. Lett.* **111**, 012001 (2013).

[5] G. Aad *et al.* [ATLAS Collaboration], *Nucl. Phys. B* **889**, 486 (2014).

[6] E. Gotsman, *AIP Conf. Proc.* **1654**, 050004 (2015).

[7] G. Antchev *et al.* [TOTEM Collaboration], *Nucl. Phys. B* **899**, 527 (2015).

[8] M. Berretti [TOTEM Collaboration], *AIP Conf. Proc.* **1654**, 040001 (2015).

[9] G. Aad *et al.* [ATLAS Collaboration], *Eur. Phys. J. C* **72**, 1926 (2012).

[10] V. Khachatryan *et al.* [CMS Collaboration], *Phys. Rev. D* **92**, 012003 (2015).

[11] R. Ciesielski, K. Goulianos, `arXiv:1205.1446 [hep-ph]`.

[12] G. Antchev *et al.* [TOTEM Collaboration], *Phys. Rev. Lett.* **111**, 262001 (2013).

[13] T. Aaltonen *et al.* [CDF Collaboration], *Phys. Rev. D* **86**, 032009 (2012).

[14] S. Chatrchyan *et al.* [CMS Collaboration], *Phys. Rev. D* **87**, 012006 (2013).

[15] CMS Collaboration, Detector Performance Note, CMS-DP-2015/05.

[16] CMS Collaboration, CMS-PAS-FSQ-12-001.

[17] F. Abe *et al.* [CDF Collaboration], *Phys. Rev. Lett.* **81**, 5278 (1998); **80**, 1156 (1998); **74**, 855 (1995).

[18] B. Abbott *et al.* [D0 Collaboration], *Phys. Lett. B* **440**, 189 (1998); **76**, 734 (1996); *Phys. Rev. Lett.* **72**, 2332 (1994).

[19] J. Bjorken, *Phys. Rev. D* **47**, 101 (1993).

[20] R. Enberg, G. Ingelman, L. Motyka, *Phys. Lett. B* **524**, 273 (2002).
[21] O. Kepka, C. Marquet, C. Royon, *Phys. Rev. D* **83**, 034036 (2011).
[22] CT-PPS TDR, CERN-LHCC-2014-021, CMS-TDR-013, TOTEM-TDR-003.
[23] AFP TDR, CERN-LHCC-2015-009, ATLAS-TDR-024-2015.
[24] G. Aad *et al.* [ATLAS Collaboration], *Phys. Lett. B* **749**, 242 (2015).
[25] CMS Collaboration, CMS-PAS-FSQ-13-008.
[26] R. Aaij *et al.* [LHCb Collaboration], *J. Phys. G: Nucl. Part. Phys.* **41**, 115002 (2014).
[27] R. Aaij *et al.* [LHCb Collaboration], *J. Phys. G: Nucl. Part. Phys.* **41**, 055002 (2014).
[28] B. Abelev *et al.* [ALICE Collaboration], *Phys. Rev. Lett.* **113**, 232504 (2014).
[29] R. Aaij *et al.* [LHCb Collaboration], *J. High Energy Phys.* **1509**, 084 (2015).
[30] B. Abelev *et al.* [ALICE Collaboration], *Phys. Lett. B* **718**, 1273 (2013).
[31] B. Abelev *et al.* [ALICE Collaboration], *Eur. Phys. J.* **C73**, 2617 (2013).
[32] CMS Collaboration, CMS-PAS-HIN-12-009.
[33] B. Abelev *et al.* [ALICE Collaboration], CERN-PH-EP-2015-082.